Composites Part B 95 (2016) 453–461

Contents lists available at ScienceDirect

Composites Part B

journal homepage: www.elsevier.com/locate/compositesb

Sound absorption enhancement using solid–solid interfaces in a non-porous cement-based structural material

Po-Hsiu Chen, Chi Xu, D.D.L. Chung*

Composite Materials Research Laboratory, University at Buffalo, State University of New York, Buffalo, NY 14260-4400, USA

ARTICLE INFO

Article history:
Received 16 April 2015
Received in revised form
3 December 2015
Accepted 5 April 2016
Available online 12 April 2016

Keywords:
A. Ceramic-matrix composites (CMCs)
B. Interface/interphase
B. Internal friction/damping
C. Analytical modeling

ABSTRACT

This work shows that solid–solid interfaces in a non-porous stiff material can enhance the sound absorption and provides an analytical model for describing the effects of constituents and interfaces on the sound absorption. The sound absorption coefficient α, the propagation constant Γ and the reflectivity R were determined for cement-based materials. At 125–500 Hz, α ranges from 0.039 to 0.160; Γ ranges from 2.6×10^{-4}/mm to 3.5×10^{-4}/mm; $R > 0.9$. Silica fume (~0.1 μm) provides interfaces, thereby enhancing α and Γ by 40% and 20% respectively for cement paste (125 Hz), but it does not affect R.

1. Introduction

Sound absorption is needed to alleviate the noise pollution that increasingly erodes the quality of life of most people, particularly those in urban areas and those that work in noisy environments. Transportation (rail, highway and aircraft) is a significant source of outdoor noise.

A common mechanism of sound absorption is the viscous deformation of the solid in response to the sound wave [1–7]. Other mechanisms are the air vibration associated with the sound causing friction between the air and the pore wall of the solid and the multiple reflections of the sound at the wall of the pores [1–7]. The multiple reflections result in the sound traveling for multiple times in various directions in the material, thereby providing an additional mechanism of sound absorption. Sound absorption materials are thus commonly porous soft materials, such as foams [1–7] and textiles [8,9]. Less commonly, biomaterials [7,10] are exploited. The porosity and softness are not desirable for the structural performance.

The most established method of enhancing the sound absorption effectiveness of a material involves the introduction of porosity [1–7], though this is typically at the expense of the mechanical performance. In contrast, this paper investigates the use of solid–solid interfaces in a non-porous material to enhance the sound absorption effectiveness. Although this paper uses cement-based materials to demonstrate the concept of using solid–solid interfaces to enhance sound absorption, the method described in this paper is expected to be applicable to other materials that contain solid–solid interfaces.

From the practical viewpoint, this paper concerns sound absorption materials that are stiff and non-porous, due to the interest in sound absorption materials that are good structural materials. This interest is partly because such a structural material would reduce or even eliminate the need for the use of a soft non-structural sound absorption material in combination of a structural material in order to render sound absorption capability to a structure. This would simplify design and avoid the bulkiness and extra weight associated with the presence of the soft sound absorption material. Furthermore, a structural material tends to be more durable than a soft material. In addition, the large volume of a structural material in a structure enables the structural material to have a large influence on the sound absorption ability of the structure.

Cement-based materials with improved effectiveness for sound absorption are commonly porous [11–17], with the pores introduced by the use of admixtures (e.g., perlite [8]), aggregates, foaming agents or templating methods. Another approach involves

* Corresponding author. Tel.: +1 716 645 3977; fax: +1 716 645 2883.
E-mail addresses: pc59@buffalo.edu (P.-H. Chen), monicachixu@gmail.com (C. Xu), ddlchung@buffalo.edu (D.D.L. Chung).
URL: http://alum.mit.edu/www/ddlchung

http://dx.doi.org/10.1016/j.compositesb.2016.04.024
1359-8368/

the incorporation of non-porous admixtures (e.g., cellulose fibers) that inherently have some viscous character [18,19].

The internal solid–solid interfaces in a non-porous solid are to be distinguished from the air–solid interface associated with a porous solid [1–7]. Prior work on sound absorption has emphasized the latter. In contrast, this work uses the solid–solid interfaces in a non-porous cement-based material to enhance the sound absorption effectiveness.

By incorporating silica fume as an admixture in the cement-based material, a large amount of interface area per unit volume is obtained. Silica fume is submicron silica (SiO_2) particles. It is a waste material and a pozzolanic admixture for enhancing the mechanical properties and decreasing the liquid permeability of cement-based materials [20]. These effects relate to the microstructural refinement, which also results in enhanced bonding with steel [21].

Silica fume tends to increase the vibration damping ability of cement-based materials [22]. The damping improvement is attributed to the low-amplitude dynamic slippage that occurs at the interface between silica and the cement matrix during vibration [22]. Damping relates to the viscous behavior, which promotes the sound absorption ability. The effect of silica fume on the sound absorption ability has not been previously addressed, though silica fume was used as an admixture along with perlite for improving the sound absorption ability of cement [15].

Silane acts as a coupling agent between silica and cement. It consists of molecules, with each molecule having desired functional groups at its two ends [23]. Silane treatment has been shown to improve the effectiveness of silica fume for promoting the vibration damping ability of cement-based materials [22], due to the viscous character of the silane molecules and the effect of the silane treatment on the interface between cement and a silica fume particle. Therefore, both silane-treated silica fume and untreated silica fume are used in this work.

Sound intensity (I, in W/m^2) is defined as the sound power per unit area. It is the product of the sound pressure (root mean square sound pressure, in Pa) and the particle velocity (in m/s). For a plane progressive wave, I is given by

$$I = p^2 \Big/ Z, \tag{1}$$

where p is the sound pressure and Z is the characteristic acoustic impedance. In this context, the phase of the sound wave is not considered [24]. The sound absorption coefficient (α) of a material is a quantity that describes how much of the incident sound intensity is not reflected by the material. It is defined as

$$\alpha = I_a / I_i \tag{2}$$

where I_a is the unreflected sound intensity and I_i is the incident sound intensity. Although α values as high as 1.0 have been reported [8], the high values are achieved only over narrow frequency ranges [15].

Although α has been reported for a number of cement-based materials [11–19], the contributions of the various constituents (including the interfaces) to α have not been elucidated. Knowledge of these contributions is valuable for guiding the design of cement-based materials for sound absorption. By systematically measuring α of cement paste, mortar (with fine aggregate, i.e., sand) and concrete (with fine and coarse aggregates, i.e., sand and stones), each with and without silica fume, this work provides the first determination of the contributions of the various constituents and interfaces on α of cement-based materials.

Ultrasound is sound with a frequency above the upper limit of human hearing (i.e., >20 kHz). Typically investigated ultrasonic frequencies exceed 1 MHz. Due to the importance of medical ultrasonography and ultrasonic testing, ultrasonic absorption [25–29] has received much more attention than the absorption of audible sound. Due to medical ultrasonography, most work on ultrasonic absorption is concerned with liquids [25–27], e.g., ferrofluids with $\Gamma = 0.28$/mm at 3.6 MHz [25]. In contrast, this work is limited to sound in the audible range (125–500 Hz).

The objectives of this work are (i) to investigate the use of solid–solid interfaces in a non-porous material to enhance the sound absorption effectiveness, (ii) to provides an analytical model for describing the effects of solid constituents and solid–solid interfaces on the sound absorption, (iii) to investigate and determine the contributions of cement, silica fume and aggregates on the sound absorption coefficient of cement-based materials without introduced porosity, (iv) to characterize the sound absorption behavior of cement-based materials at a level beyond that of prior work, (v) to develop cement-based materials that exhibit enhanced sound absorption without loss of strength due to porosity, and (vi) to strengthen the science base for the design of materials for sound absorption.

2. Methods

The value of α can be measured by either the reverberation chamber method (ASTM C423, also known as the room method) or the impedance tube method (ASTM E1050). In the room method, the sound absorption material under test lines all the surfaces of the room and a diffuse sound field is used, so that the sound has evenly distributed angles of incidence relative to the surfaces of the test material. The room method is commonly used for commercial product evaluation. In the impedance tube method [8,24], sound is emitted from one end of a hollow tube, with the test specimen at the other end of the tube, so that α is measured at normal incidence. This method is commonly used for research and is used in this work.

Upon the incidence of a sound wave on to a solid surface, a part of the sound intensity is reflected by the surface whereas the remaining part enters the solid and becomes absorbed as it travels into the solid. The extent of reflection of the sound at the front and back surfaces of the solid and the extent of absorption of the sound within the thickness of the solid are fundamental to understanding the interaction of sound with the solid. However, this information has not been previously reported in relation to cement-based materials. By measuring α for various thicknesses of the material, this work provides the first determination of the reflectivity R (the fraction of incident sound intensity that is reflected at a surface) and the propagation constant Γ (the distance in the material over which the sound intensity is reduced by absorption by a factor of 1/e) of cement-based materials. The quantity Γ is defined by the equation

$$I = I_o\, e^{-\Gamma x}, \tag{3}$$

where I_o is the incident sound intensity and I is the sound intensity at a distance x beneath the surface of the solid. The absorption loss in dB is given by

$$\begin{aligned} \text{Absorption loss (dB)} &= -20 \log e^{-\Gamma x} \\ &= (20/2.3)\Gamma x. \end{aligned} \tag{4}$$

The Γ is scientifically more meaningful than α, because α depends on both the material and the distance. Values of the parameters Γ and R are practically valuable, as they allow calculation

of the reflected and absorbed sound intensities for various thicknesses of the sound absorber. In this work, α, Γ and R are reported for cement-based materials.

2.1. Analytical methods

The α value of the cement part of mortar or concrete is taken as the measured α value of cement paste α_P. The α values of the interior of each sand particle, each stone particle and each silica fume particle are considered to be negligible, due to the high stiffness of these particles. Let the areal sound absorption coefficient (referring to α divided by the interface area per unit volume and having unit mm^{-1}) of the cement–sand interface, cement–stone interface and cement–silica-fume interface be γ_{PS}, γ_{PT} and γ_{PF} respectively.

Based on the Rule of Mixtures, the α value α_M of mortar without silica fume is given by

$$\alpha_M = V_P\alpha_P + A_{PS}\gamma_{PS}, \tag{5}$$

where V_P is the volume fraction of cement paste in the mortar and A_{PS} is the cement–sand interface area per unit volume in the mortar. Similarly, the α value α_C of concrete without silica fume is given by

$$\alpha_C = V_P\alpha_P + A_{PS}\gamma_{PS} + A_{PT}\gamma_{PT}, \tag{6}$$

where A_{PT} is the cement–stones interface area per unit volume.

In the presence of silica fume, the α value α_P' of the cement paste is given by

$$\alpha_P' = V_P\alpha_P + A_{PF}\gamma_{PF}, \tag{7}$$

where A_{PF} is the cement–silica-fume interface area per unit volume in the cement paste. Similarly, in the presence of silica fume, the α value α_M' of mortar is given by

$$\alpha_M' = V_P\alpha_P + A_{PS}\gamma_{PS} + A_{PF}\gamma_{PF}. \tag{8}$$

Similarly, in the presence of silica fume, the α value α_C' of concrete is given by

$$\alpha_C' = V_P\alpha_P + A_{PS}\gamma_{PS} + A_{PT}\gamma_{PT} + A_{PF}\gamma_{PF}, \tag{9}$$

The values of V_P, A_{PS}, A_{PT} and A_{PF} are obtained from simple calculations based on the geometry. The values of α_P, α_M, α_C, α_P', α_M' and α_C' are measured. From Eq. (4), γ_{PS} is obtained. Then, from Eq. (5), γ_{PT} is obtained. From Eqs. (6)–(8), γ_{PF} is obtained for cement paste, mortar and concrete respectively, although γ_{PF} should not differ much among these three cases.

Using Eqs. (5)–(9), the contributions of the various constituents (including the interfaces) to α are obtained. The Rule of Mixtures was similarly applied to obtain the contributions of the various constituents to Γ.

The interaction of sound with a solid is illustrated in Fig. 1. The incident sound intensity is I. The reflectivity R_1 is the fraction of incident sound intensity I that is reflected at the front surface of the solid. Hence, the part of the sound intensity that is reflected is IR_1. This is the first wave that emerges from the front surface.

The part of the sound intensity that is not reflected is $I(1-R_1)$ and it enters the solid. It is absorbed as it travels in the solid. At the back surface of the solid of thickness x, the sound intensity is $I(1-R_1)\,e^{-\Gamma x}$. The reflectivity R_2 is the fraction of the incident sound intensity that is reflected at the back surface of the solid. Thus, the sound intensity immediately after reflection from the back surface is $R_2\,I(1-R_1)\,e^{-\Gamma x}$. After this reflection, the sound travels toward the front surface. Upon reaching the front surface, its intensity is $R_2\,I(1-R_1)\,e^{-2\Gamma x}$. This is the second wave that emerges from the front surface.

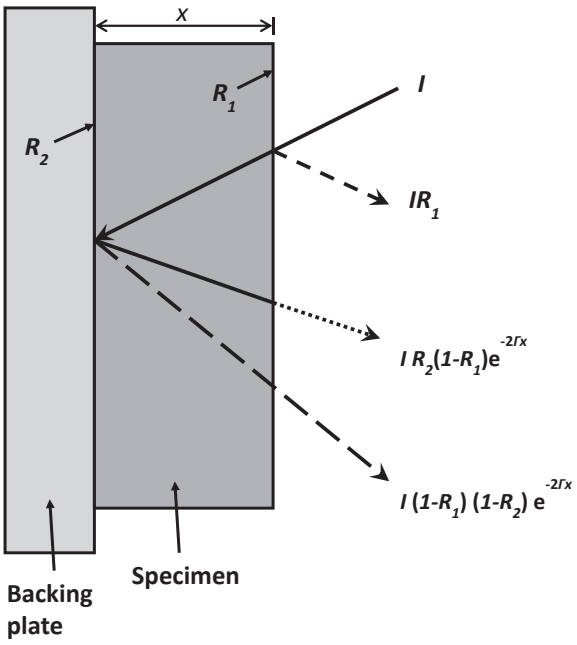

Fig. 1. Sound intensity after reflection and/or absorption. The reflectivity of the front side of the specimen is R_1; the reflectivity of the back side of the specimen is R_2. The reflectivity of the front side of the backing plate is assumed to be 100%.

At the back of the solid is a heavy metal plate that is considered to be a perfect reflector of sound. The wave that reaches this plate has intensity equal to the leftover of the intensity after reflection from the back surface of the solid. Its intensity is thus

$$I(1-R_2)(1-R_1)\,e^{-\Gamma x}.$$

Since the backplate is a perfect reflector, all of this intensity is reflected by the backplate. After the reflection, the sound enters the solid and is absorbed as it travels in the solid. When it reaches the front surface of the solid, the sound intensity is

$$I(1-R_2)(1-R_1)e^{-2\Gamma x}.$$

This is the third wave that emerges from the front surface.

The total sound intensity that emerges from the front surface is given by the sum of the contributions by the three waves mentioned above, i.e.,

$$I\left[R_1 + R_2(1-R_1)e^{-2\Gamma x} + (1-R_2)(1-R_1)e^{-2\Gamma x}\right].$$

Dividing this by I gives the fraction of incident intensity that emerges from the front surface. This fraction is known as the sound intensity reflection coefficient R^*, which is equal to 1 minus the fraction of incident intensity that is unreflected (α). Hence,

$$1-\alpha = R_1 + R_2(1-R_1)e^{-2\Gamma x} + (1-R_2)(1-R_1)e^{-2\Gamma x}. \tag{10}$$

In the idealistic case in which $\alpha = 1$, both R_1 and R_2 are equal to zero, and $\Gamma x = \infty$, according to Eq. (10). Hence, α being high means that Γx is high and does not imply that Γ is high.

Experimentally, α is measured. There are three unknowns in Eq. (10), namely R_1, R_2 and Γ. By measuring α for three thicknesses (i.e., three values of x), one obtains three equations, which can be solved simultaneously to determine the three unknowns.

2.2. Experimental methods

2.2.1. Materials

Portland cement (Type I, ASTM C150) with true density 3.15 g/cm^3 was used. Silica fume (if used) was at 15% by mass of cement, as in prior work [22]. Its true density was 2.22 g/cm^3. It had a particle size ranging from 0.03 to 0.5 μm, with an average size of 0.2 μm; the particles tended to form clusters of typical size around 20 μm. It contained >93 wt.% SiO_2, <0.7 wt.% Al_2O_3, <0.7 wt.% CaO, <0.7 wt.% MgO, <0.5 wt.% Fe_2O_3, <0.4 wt.% Na_2O, <0.9 wt.% K_2O, and <6 wt.% loss on ignition. The true density was 2.1 g/cm^3.

The silane coupling agent was a 1:1 (by weight) mixture of Z-6020 and Z-6040 (Dow Corning, Midland, MI) [15]. The amine group in Z-6020 served as a catalyst for the curing of the epoxy and consequently allowed the Z-6020 molecule to attach to the epoxy end of the Z-6040 molecule. The trimethylsiloxy ends of the Z-6020 and Z-6040 molecules then connected to the −OH functional group on the surface of the silica fume. The silane was dissolved in ethylacetate. The concentration of silane in the ethylacetate solution was varied from 0.5% to 5.0 wt.%. Surface treatment of the silica fume was performed by immersion in the silane solution, heating to 75 °C while stirring, and then holding at 75 °C for 1.0 h, followed by filtration and drying. After this, the silica fume was heated at 110 °C for 12 h.

The fine aggregate was natural sand with true density 2.65 g/cm^3 and a typical particle size of approximately 0.3 mm. The sand-cement ratio was 1.00. The coarse aggregate (stones) had true density 2.65 g/cm^3 and a typical particle size of 2.0 mm. The mass ratio of cement: sand: stones in concretes was 1:1.5:2.5. The water–cement ratio (W/C) was 0.35 for cement pastes without silica fume, 0.40 for cement pastes with silica fume, and 0.45 for all mortars and concretes. A high-range water-reducing agent (Glenium 3000NS, BASF Construction Chemicals) was used at 1.0% by mass of cement. The defoamer (Colloids Inc., Marietta, GA, 1010) was used at 0.13% (percent of specimen volume).

2.2.2. Testing methods

For sound absorption testing, the specimens were square, of size 145 × 145 mm and nominal thickness 24, 62 or 99 mm; the exact thickness was measured separately for each specimen tested. All ingredients were mixed in a rotary mixer with a flat beater for 5 min. After pouring into molds, an external vibrator was used for 3 min to facilitate compaction and decrease the amount of air bubbles. The specimens were demolded after 24 h and then cured in air at room temperature and a relative humidity of 100% for 28 days. Three specimens of each type were tested.

The normal-incidence sound absorption coefficient is more useful than the random-incidence coefficient for the purpose of material behavior characterization, and is particularly valuable for predicting the effect of placing a material in a small enclosed space. This work concerns testing under normal incidence.

For the sound absorption testing, the impedance tube method (ASTM C384-04) was used (Fig. 2(a)). The cylindrical tube was aluminum (Type 6061, with wall thickness 6.4 mm), reinforced on its outer surface with epoxy-impregnated continuous carbon fiber ribbon (3.2 mm wide) that was wound around the perimeter of the tubing along its entire length. The fiber (Thornel P-25X, Cytec Industries Inc., Woodland Park, NJ) was continuous and pitch-based. The tube was 3.676 m long, 114.3 mm in outer diameter and 101.6 mm in inner diameter. The specimen was positioned at one end of the tube, while loudspeakers were positioned at the other end. A square steel (Type 1045) backing plate of thickness 25.4 mm was held by fastening and a rubber O-ring (not shown in Fig. 2(a)) at the back of the specimen, such that it extended beyond the four edges of the square specimen. A square steel frame was fitted around the four edges of the specimen in order to avoid sound leakage to the environment from the edges of the specimen. The specimen was fastened to the end of the impedance tube with the help of a rubber O-ring (not shown in Fig. 2(a)). Four small cylindrical loudspeakers were positioned in four circular holes (diameter 44.5 mm) that had been drilled though an aluminum (Type 6061) plate of thickness 12.7 mm, such that they were symmetrically positioned relative to the cylindrical axis of the impedance tube. Software (TrueRTA, v. 3.5.2, True Audio, Andersonville, TN) was used with a Personal Computer to generate sound at the frequency of 125, 250 or 500 Hz. With the impedance tube of length 3.676 m and the speed of sound in dry air being 343 m/s (http://en.wikipedia.org/wiki/Speed_of_sound, as viewed on July 24, 2014), the frequency of 125 Hz corresponds to 1.3 wavelength along the length of the tube and the frequency of 500 Hz corresponds to 5.4 wavelengths along the length of the tube. The frequency range studied in this work is from 125 to 500 Hz.

A sliding steel tubing with outer diameter 19.1 mm and inner diameter 17.1 mm was held in a hole of diameter 19.1 mm at the center of the plate holding the loudspeakers (Fig. 2(b)), such that this hole was centered at the axis of the impedance tube. This tubing had a microphone (Model BY-A01, BOYA Audio Equipment Co., Shenzhen, China) mounted at its end and an electrical lead from the microphone inside the tubing. Four spiders (not shown in Fig. 2(a)) were installed inside the tube and spaced along the length of the tube so as to align the microphone and the centerline of the tube. The sound wave which is absorbed by the spider can be neglected due to its small surface area. The sliding tubing was positioned at the cylindrical axis of the impedance tube, such that it could be moved manually along the axis of the impedance tube. In order to observe the standing sound wave in the impedance tube, microphone voltage data were collected at various distances from the specimen surface, such that the points of data collection were 25.4 mm apart along the axis of the impedance tube. Both the output and input signals were fed to a signal conditioner (PCB Piezotronics, Inc., Depew, NY, Model 483AO7) in order to reduce the noise.

The α values obtained using this testing system are in line with values that have been previously reported for various materials, particularly cement-based materials. This supports the validity of the testing method.

Sound emitted by the loudspeakers was partly reflected by the specimen and partly absorbed by the specimen. In a separate experiment involving specimens of nominal thickness 25.4, 63.5 and 101.6 mm, it was found that a nominal thickness of 63.5 mm was adequate. Nevertheless, in case of cement pastes, testing was performed for all three thicknesses in order to decouple the absorption and reflection effects.

The sound intensity reflection coefficient R^* is related to the sound pressure reflection coefficient (r) by the equation

$$R^* = r^2. \tag{11}$$

Since $R^* = 1 - \alpha$, by definition, Eq. (11) gives

$$\alpha = 1 - r^2. \tag{12}$$

The standing wave ratio (S) is defined as

$$S = V_{max}/V_{min}, \tag{13}$$

where V_{max} and V_{min} are respectively the maximum and minimum voltages in the standing wave detected by the microphone.

The sound pressure reflection coefficient r relates to the standing wave ratio (S) by the equation [30].

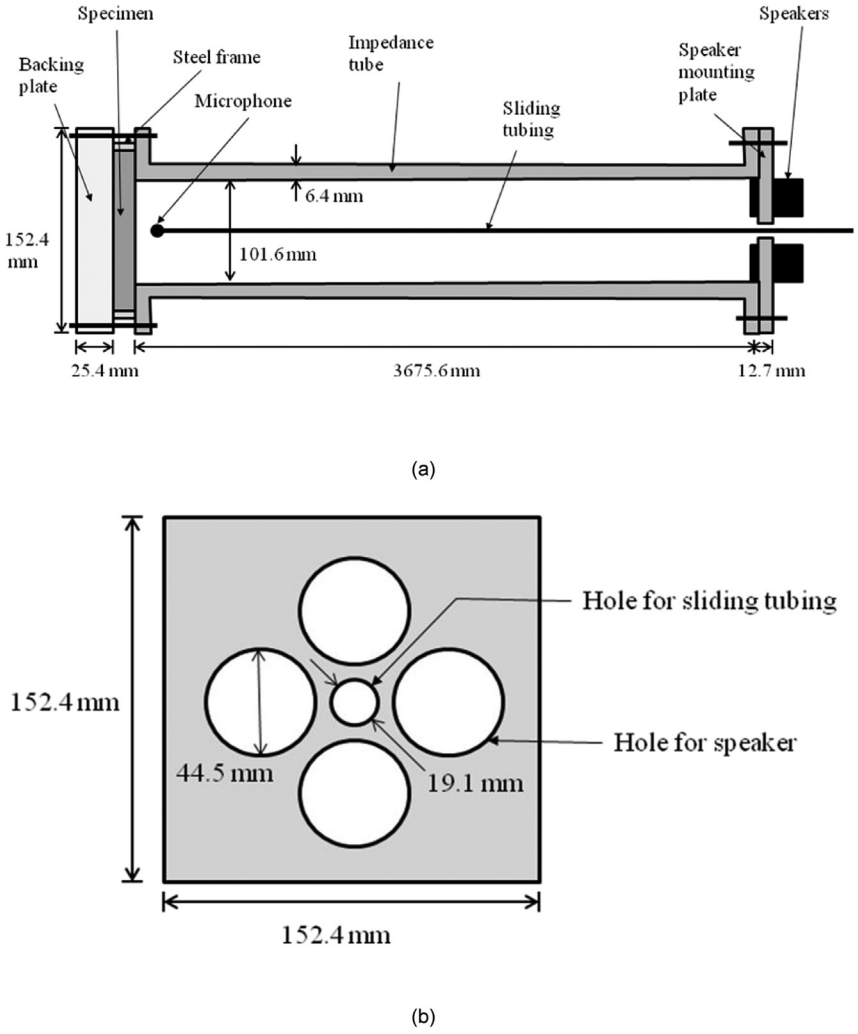

Fig. 2. Experimental set-up for sound absorption testing using the impedance tube method. (a) Overall set-up. Due to the long length of the impedance tube, the drawing is not to scale. (b) The speaker mounting plate located at the right end of the impedance tube in (a).

$$r = (S-1)/(S+1). \quad (14)$$

By measuring S and using Eqs. (12) and (14), α is determined.

3. Results and discussion

Table 1 shows the values of α at 125 Hz. The addition of silica fume increases α substantially. The effect is similar for untreated silica fume and silane-treated silica fume, as shown for cement paste. The fractional increase in α due to the silica fume addition is similar for cement paste and mortar, but is higher for concrete. The α value is similar for cement paste and mortar (both 0.07 in the absence of silica fume), but is lower for concrete (0.04 in the absence of silica fume).

Table 2 shows the effect of frequency (125–500 Hz) and specimen thickness on α for cement paste with and without silane-treated silica fume. The α value increases slightly with increasing frequency, as expected, whether silica fume is present or not. It increases with increasing thicknesses, as expected.

Table 3 shows the values of R_1, R_2 and Γ calculated from the measured α of cement paste with and without silane-treated silica fume. Both R_1 and R_2 are high, exceeding 0.9, such that R_2 is slightly

Table 1
Sound absorption coefficient α at 125 Hz, obtained for nominal specimen thickness 62 mm, such that the exact thickness was measured separately for each specimen tested.

Material	Silica fume	α	Fractional increase in α due to silica fume
Cement paste	None[a]	0.072 ± 0.004	/
	Untreated	0.094 ± 0.006	(31 ± 6)%
	Silane-treated	0.101 ± 0.009	(40 ± 7)%
Mortar	None[a]	0.070 ± 0.007	/
	Silane-treated	0.090 ± 0.005	(29 ± 5)%
Concrete	None[a]	0.044 ± 0.005	/
	Silane-treated	0.075 ± 0.008	(70 ± 9)%

[a] Without silica fume.

Table 2
Sound absorption coefficient α of cement pastes at different frequencies, obtained for three nominal specimen thicknesses (24, 62 and 99 mm), such that the exact thickness was measured separately for each specimen tested.

Silica fume	Thickness (mm)	α		
		125 Hz	250 Hz	500 Hz
None[a]	23.6 ± 0.8	0.039 ± 0.003	0.044 ± 0.004	0.059 ± 0.005
	61.7 ± 1.1	0.072 ± 0.004	0.082 ± 0.005	0.092 ± 0.006
	98.6 ± 0.9	0.095 ± 0.006	0.109 ± 0.007	0.113 ± 0.006
Silane-treated	23.9 ± 0.7	0.061 ± 0.007	0.068 ± 0.006	0.081 ± 0.007
	61.5 ± 0.8	0.101 ± 0.009	0.120 ± 0.011	0.141 ± 0.010
	99.2 ± 1.0	0.124 ± 0.011	0.137 ± 0.012	0.160 ± 0.014

[a] Without silica fume.

Table 3
Parameters R_1, R_2 and Γ determined from the measured sound absorption coefficient α of cement paste for three nominal specimen thicknesses (24, 62 and 99 mm), such that the exact thickness was measured separately for each specimen tested.

	Silica fume	125 Hz	250 Hz	500 Hz
R_1	None	0.904 ± 0.013	0.925 ± 0.008	0.936 ± 0.007
	Silane-treated	0.895 ± 0.004	0.911 ± 0.004	0.920 ± 0.005
R_2	None	0.993 ± 0.003	0.994 ± 0.003	0.996 ± 0.003
	Silane-treated	0.991 ± 0.005	0.993 ± 0.004	0.995 ± 0.003
Γ (10^{-4}/mm)	None	2.21 ± 0.19	3.07 ± 0.23	3.23 ± 0.29
	Silane-treated	2.61 ± 0.20	3.35 ± 0.24	3.51 ± 0.25
Fractional increase in Γ due to silica fume		(18 ± 6)%	(9.1 ± 3.0)%	(8.7 ± 2.7)%

higher than R_1 and the presence of silica fume has negligible effect on both R_1 and R_2. That R_2 is slightly higher than R_1 probably relates to the steel backplate that is almost in contact with the back side of the specimen (due to the O-ring at the interface) and the high reflectivity of the backplate. The value of R_1 increases slightly with increasing frequency, whereas that of R_2 does not change with the frequency. That R_2 does not change with the frequency is consistent with the notion that the steel backplate affects R_2. The Γ increases with increasing frequency and is higher when silica fume is present.

The presence of silica fume increases Γ by about 20% for cement paste at 125 Hz (Table 3), whereas it increases α by 40% for cement paste at the same frequency (Table 1). These increases due to silica fume addition are attributed to the small size of the silica fume clusters (Table 8) and the consequent large area of the interface between the silica fume clusters and cement and the resulting multiple reflections at these interfaces. These interfaces also contribute to enhancing the degree of viscous character, which provides an additional mechanism of sound absorption. The viscous character enhancement due to the silica fume addition has been previously reported, based on dynamic mechanical analysis [21,22]. The analytical model of this work does not distinguish between these two mechanisms of sound absorption. That the fractional increase in Γ is relatively small compared to the fractional increase in α probably relates to the fact that Γ is in the exponent in Eq. (3), whereas α is not in the exponent (Eq. (2)). In spite of the increase in Γ with increasing frequency, the fractional increase in Γ due to the silane-treated silica fume addition is greater at 125 Hz than 250 or 500 Hz (Table 3).

The highest value of Γ achieved in this work is 3.5×10^{-4}/mm (Table 3). With this value of Γ, the distance x needs to be 6.6 m in order to achieve an absorption loss of 20 dB, according to Eq. (4). Since the sound wave travels inward and then outward through the thickness of the absorber, the thickness of the absorber needs to be (6.6 m)/2 = 3.3 m, which is very large.

In Table 4, columns 2–4 correspond to the three terms on the right side of Eq. (10) and describe respectively the intensity R_1 upon reflection from the front surface, the intensity $R_2\,(1 - R_1)\,e^{-2\Gamma x}$ that emerged after reflection from the back surface of the specimen, and the intensity $(1 - R_2)\,(1 - R_1)\,e^{-2\Gamma x}$ that emerged after reflection from the front surface of the backing plate. The last column R^* in Table 4 describes the total intensity that emerged from the front surface of the specimen, relative to the incident intensity. The R^* is high, exceeding 0.94. Moreover, it decreases with increasing frequency, as expected due to the increase of α with increasing frequency (Table 2). Table 4 also shows that R^* is dominated by the contribution R_1 from the reflection from the front surface of the specimen. The value of R_1 exceeds 0.9 and increases slightly with increasing frequency. The contribution $R_2\,(1 - R_1)\,e^{-2\beta x}$ from the reflection from the back surface of the specimen is very small. In addition, it decreases with increasing frequency, due to Γ increasing with increasing frequency (Table 3). The contribution $(1 - R_2)\,(1 - R_1)\,e^{-2\Gamma x}$ from the front surface of the steel backplate is negligible.

Tables 5 and 6 show the fractional contributions of the various constituents (including interfaces) in the cement-based material to α and Γ respectively. In relation to α, the fractional contributions are obtained by calculation using Eqs. (5)–(9) and the geometry-related parameters shown in Tables 7 and 8. In relation to Γ, the fractional contributions are similarly obtained. As shown in Tables 5 and 6, the interface between silica fume and cement is the primary contributor to α and Γ whenever silica fume is present, whether aggregates are present or not.

For cement paste, silica fume and cement contribute about equally to α or Γ, such that the silica fume contribution is slightly higher than the cement contribution. The significant contribution of cement is due to the heterogeneity in the cement and the large volume fraction V_P of the cement (Table 7). The interior of a sand or stone particle is much more uniform than the interior of cement.

For mortar, the cement–sand interface contributes to α, but this contribution is small, being 0.33 in the absence of silica fume and being 0.18 in the presence of silica fume (Table 5). That the contributor is minor is because of the large size of the sand particles (Table 8) compared to the silica fume clusters and the consequent relatively small area of the cement–sand interface. In the presence of silica fume, the contribution from the cement–sand interface (0.18) is small compared to the contribution from either cement (0.38) or the interface between cement and silica fume (0.44). In the absence of silica fume, cement is the primary contributor (0.67); in the presence of silica fume, the interface between cement and silica fume is the primary contributor (0.44).

For concrete, the cement–stones interface contributes to α by a very small degree (ranging from 0.05 to 0.09, Table 5), because of the large size of the stones (Table 8) and the consequent small area of the cement–stones interface. Cement is the primary contributor (0.53) in the absence of silica fume and the interface between cement and silica fume is the primary contributor (0.51) in the presence of silica fume (Table 5).

Table 6 shows that the interface of the cement with the silica fume clusters is the primary contributor to Γ when silica fume is

Table 4
The contributions to the sound intensity that emerges from the front surface of the specimen of thickness 24 mm, such that the exact thickness was measured separately for each specimen tested. No silica fume is present. All quantities are relative to the incident intensity.

Frequency (Hz)	From front surface of specimen R_1	From back surface of specimen $R_2\,(1-R_1)\,e^{-2\Gamma x}$	From front surface of the backing plate $(1-R_2)\,(1-R_1)\,e^{-2\Gamma x}$	R^*
125	0.904 ± 0.004	0.056 ± 0.002	0.001 ± 0.000	0.961 ± 0.003
250	0.925 ± 0.004	0.031 ± 0.001	<0.0001	0.956 ± 0.004
500	0.936 ± 0.005	0.005 ± 0.000	<0.0001	0.941 ± 0.005

Table 5
Fractional contributions to the sound absorption coefficient α by various components, which include the cement, the cement–sand interface, the cement–stones interface and the cement–silica-fume interface at 125 Hz.

Silica fume status	Cement paste			Mortar		Concrete	
	None	Untreated	Silane-treated	None	Silane-treated	None	Silane-treated
Cement	1.000	0.476 ± 0.003	0.447 ± 0.003	0.672 ± 0.013	0.377 ± 0.002	0.527 ± 0.002	0.259 ± 0.001
Cement–sand interface	0	0	0	0.328 ± 0.013	0.183 ± 0.019	0.384 ± 0.016	0.189 ± 0.018
Cement–stones interface	0	0	0	0	0	0.0890 ± 0.0016	0.0455 ± 0.0110
Cement–silica-fume interface	0	0.524 ± 0.003	0.553 ± 0.003	0	0.441 ± 0.019	0	0.508 ± 0.030

Table 6
Fractional contributions to the propagation constant Γ of cement paste by various constituents, which include the cement, the cement–sand interface, the cement–stones interface and the cement–silica-fume interface at 125 Hz.

Silica fume status	None[a]	Untreated	Silane-treated
Cement	1.00 ± 0.00	0.44 ± 0.01	0.40 ± 0.02
Cement–silica-fume interface	0	0.54 ± 0.01	0.60 ± 0.02

[a] Without silica fume.

Table 7
Values of the volume fraction V_P of cement paste, as calculated based on the masses and densities of the ingredients.

Cement paste		Mortar		Concrete	
No[a]	Yes[b]	No[a]	Yes[b]	No[a]	Yes[b]
1.000	0.627	0.651	0.472	0.322	0.270

[a] Without silica fume.
[b] With silane-treated silica fume.

Table 9
Parameters describing the extent of interaction of sound (125 Hz) with various constituents, which include the cement (α_P and β_P), the cement–sand interface (γ_{PS}), the cement–stones interface (γ_{PT}), and the cement–silica-fume interface (γ_{PF}).

α_P[a]		0.072 ± 0.004
$\Gamma_P\,(10^{-4}/\text{mm})$[b]		2.21 ± 0.19
γ_{PS} (mm)		0.0033 ± 0.0002
γ_{PT} (mm)		0.0031 ± 0.0004
$\gamma_{PF}\,(10^{-4}$ mm)[c]	Cement paste	5.04 ± 0.50
	Mortar	4.78 ± 0.65
	Concrete	7.92 ± 1.18

[a] The α value of cement paste without silica fume; from Table 1.
[b] The Γ value of cement paste without silica fume; from Table 3.
[c] Silane-treated silica fume.

Table 8
Values of the interface area per unit volume, calculated based on the particle size of sand for the cement–sand interface, the particle size of stones for the cement–stones interface and the aggregate size of silica fume for the cement–silica-fume interface. These values are needed for the analytical modeling.

Interface area per unit volume (mm^{-1})	Particle size	Cement paste	Mortar		Concrete	
		Yes[b]	No[a]	Yes[b]	None[a]	Yes[b]
A_{PS}	0.30 ± 0.03 mm	0	7.01 ± 0.70	4.98 ± 0.50	5.09 ± 0.51	4.28 ± 0.42
A_{PT}	2.0 ± 0.4 mm	0	0	0	1.27 ± 0.25	1.07 ± 0.21
A_{PF}	20 ± 2 μm[c]	112 ± 11	0	84.2 ± 8.4	0	48.4 ± 4.8

[a] Without silica fume.
[b] With silane-treated silica fume.
[c] Cluster size rather than particle size.

present. The fractional contribution is higher for silane-treated silica fume than untreated silica fume. These results on β are consistent with those on α (Table 5).

Table 9 shows the values of the parameters that are used in calculating the contributions of the various constituents to α (Table 5) and Γ (Table 6) at 125 Hz. The effectiveness γ_{PF} of the interface (per unit of the interface area per unit volume) between cement and silica fume is small and similar for cement paste, mortar and concrete. The effectiveness γ_{PS} of the cement–sand interface and the effectiveness γ_{PT} of the cement–stones interface are similarly much higher than that of the interface between cement and silica fume. The low effectiveness of the interface between cement and silica fume is attributed to the small size of the silica fume clusters and the consequent absence of an effective reflection surface. In spite of its low effectiveness per unit of the interface area per unit volume, the interface between cement and silica fume is the primary contributor to α (Table 5) or Γ (Table 6). This is because of the large interface area per unit volume of this interface. In contrast, the effectiveness (per unit of the interface area per unit volume) of the cement–sand and cement–stones interface is relatively high, due to the relatively large sizes of the sand and stone particles for providing an effective reflection surface. However, the interfaces with sand and with stones are minor contributors to α (Table 5) and Γ (Table 6), due to the small values of their interface area per unit volume. The values of γ_{PS} and γ_{PT} are essentially the same (Table 9). The values of γ_{PF} obtained for cement

paste, mortar and concrete are quite close (Table 9). These similarities provide further support for the validity of the analytical model (Section 2.1).

Most of the incident sound intensity is reflected from the front surface of the specimen rather than being absorbed by the interior of the specimen (Table 4). This occurs even in the presence of silica fume. The use of other admixtures, such as perlite [15], may be needed in order to increase the extent of absorption.

The important contribution of silica fume to sound absorption is consistent with the important contribution of silica fume to vibration damping [22]. For both sound absorption and vibration damping, silica fume contributes due to the large area of the interface between cement and the silica fume clusters. In sound absorption, multiple reflections occur at these interfaces. In vibration damping, slight slippage (which involves friction) occurs at these interfaces, thus resulting in mechanical energy dissipation [22].

Comparison between the effects of untreated and silane-treated silica fume shows that silane treatment of silica fume helps vibration damping [22], but has little effect on sound absorption. This is probably because the multiple reflections of sound at the interface between cement and silica fume clusters are not much affected by the presence of the silane coating on the silica fume particles, whereas the slippage at this interface is affected by the silane coating. This difference between sound absorption and vibration damping probably also relates to the fact that the frequency is 125–500 Hz for sound absorption evaluation (this work) and only 0.2 Hz for vibration damping evaluation [22]. The low frequency in damping evaluation makes the viscoelastic effect of the silane more influential.

The highest value of α obtained in this work is only 0.160 (500 Hz, Table 2), which is low compared to most conventional sound absorption materials. For example, at 500 Hz, a 25-mm glass fiber board exhibits $\alpha = 0.75$ [31]. Nevertheless, the fractional increase in α due to silica fume addition is up to 70%. Most importantly, this work provides the scientific base for the use of solid–solid interfaces to enhance sound absorption. With the use of nanotechnology, such as nanofillers, the amount of solid–solid interface area per unit volume may be increased, thereby enhancing the effect of solid–solid interfaces on the sound absorption.

4. Conclusions

This work shows that solid–solid interfaces in a material can enhance the sound absorption effectiveness. In addition, this work provides an analytical model for describing the effects of solid constituents and the associated solid–solid interfaces on the sound absorption effectiveness.

Cement-based materials without introduced porosity are attractive for their high strength compared to those with porosity. This work provides new information on the extent of absorption and reflection of sound by cement-based materials without introduced porosity. The contributions of cement, aggregates, silica fume and the cement–aggregate and cement–silica-fume interfaces on the sound absorption coefficient have been decoupled and determined for the first time. The information is fundamental to understanding the interactions of sound with cement-based materials and is valuable for the design of cement-based materials for sound absorption.

This work has provided characterization of the sound absorption behavior of cement-based materials at a level beyond that of prior work. In addition to measuring the sound absorption coefficient α, this work has determined the propagation constant Γ and the reflectivity R_1 of the front surface of the material under evaluation. The method used in this work for determining Γ and R_1 involves measuring α at three different specimen thicknesses and solving three associated simultaneous equations.

In addition, this work has elucidated the contributions of the solid constituents and solid–solid interfaces of a material on the sound absorption coefficient α of cement-based materials. This elucidation is enabled by measurement of α for cement paste with and without silica fume, mortar with and without silica fume, and concrete with and without silica fume, and the use of the Rule of Mixtures. Thus, silica fume addition is found to enhance α by 40%, 30% and 70% for cement paste, mortar and concrete respectively (125 Hz). This is due to the increase of Γ, which, in the case of cement paste, is increased by the silica fume addition by 20% (125 Hz). Both α and Γ increase slightly with increasing frequency from 125 to 500 Hz. The values of α range from 0.039 to 0.160; the values of Γ range from 2.6×10^{-4}/mm to 3.5×10^{-4}/mm. Silica fume essentially does not affect R_1, which is very high (>0.9), whether silica fume is present or not.

The contribution to α decreases in the order: silica fume, cement, sand and stones. Silica fume, sand and stones contribute to α due to the reflection at the interface between these particles and cement and the consequent multiple reflections at the cement–particle interfaces. However, the increase in viscous character due to the presence of the interfaces also contributes to enhancing the sound absorption. When silica fume is present, it is the primary contributor, with its contribution ranging from 44% to 55%, and cement is the second greatest contributor, with its contribution ranging from 26% to 48%. When sand is present, its contribution ranges from 18% to 33%. When stones are present, their contribution ranges from 4.7% to 9.1%.

Acknowledgment

The authors thank Professor Andres Soom of University at Buffalo, State University of New York, for allowing them to use his signal conditioner. They are also thankful to the Center for Undergraduate Research & Creative Activities and the Graduate Student Association (Mark Diamond Research Fund) of the same university for partial funding of this work.

References

[1] Subramonian S, Remy L, Schroer D. Acoustics and forming of novel polyolefin blend foams. Cell Polym 2004;23(6):349–67.
[2] Banhart J. Industrialisation of aluminium foam technology. Mater Forum 2004;28:764–70.
[3] Madigosky WM, Harrison RW, Scharnhorst KP. Effect of air inclusions on absorption and velocity of sound in viscoelastic materials. Polym Mater Sci Eng 1989;60:489–96.
[4] Imai Y. Studies of acoustical absorption of flexible polyurethane foam. Acoust Lett 1982;5(9):141–3.
[5] Fei YN, Khan AA. The effect of sound absorption coefficient of particle addition to polyurethane matrix composites. Aust J Basic Appl Sci 2014;8(spec. iss. 15): 246–51.
[6] Lu TJ, Chen F, He D. Sound absorption of cellular metals with semiopen cells. J Acoust Soc Am 2000;108(4):1697–709.
[7] Zhu X, Kim B, Wang Q, Wu Q. Recent advances in the sound insulation properties of bio-based materials. BioResources 2014;9(1):1–23.
[8] Lee YE, Joo CW. Sound absorption properties of thermally bonded nonwovens based on composing fibers and production parameters. J Appl Polym Sci 2004;92(4):2295–302.
[9] Soltani P, Zerrebini M. The analysis of acoustical characteristics and sound absorption coefficient of woven fabrics. Text Res J 2012;82(9):875–82.
[10] Jayamani F, Hamdan S, Rahman MR, Bin Bakri MK, Kakar A. An investigation of sound absorption coefficient on sisal fiber poly lactic acid bio-composites. J Appl Polym Sci 2015;132(34).
[11] Neithalath N, Weiss J, Olek J. Acoustically efficient concretes through engineered pore structure. In: Autoclaved aerated concrete: properties and structural design, vol. SP-226. American Concrete Institute, SP; 2005. p. 135–47.

[12] Ferrándiz-Mas V, García-Alcocel E. Physical and mechanical characterization of Portland cement mortars made with expanded polystyrene particles addition (EPS). Mater Constr 2012;62:547–66.
[13] Kim HK, Lee HK. Influence of cement flow and aggregate type on the mechanical and acoustic characteristics of porous concrete. Appl Acoust 2010;71:607–15.
[14] Shebl SS, Seddeq HS, Aglan HA. Effect of micro-silica loading on the mechanical and acoustic properties of cement pastes. Constr Build Mater 2011;25:3903–8.
[15] Jin X, Zeng L. Sound absorption characteristics and air-flow resistivity determination of metro sound absorbed material. Rengong Jingti Xuebao 2008;37(4):918–26.
[16] Petrella A, Petrella M, Boghetich G, Petruzzelli D, Ayr U, Stefanizzi P, et al. Thermo-acoustic properties of cement-waste-glass mortars. Proc Inst Civ Eng Constr Mater 2009;162(CM2):67–72.
[17] Rutkevicius M, Mehl GH, Paunov VN. Sound absorption properties of porous composites fabricated by a hydrogel templating technique. J Mater Res 2013;28:2409–14.
[18] Neithalath N, Weiss J, Olek J. Acoustic performance and damping behavior of cellulose–cement composites. Cem Concr Compos 2004;26:359–70.
[19] Udoeyo FF, Anyanwu ClO, Brooks R, Udo-Inyang P. Properties of palm nut fiber-reinforced cement composite containing pulverized kernel shell as supplementary material. J Mater Civ Eng 2011;23:378–84.
[20] Xu Y, Chung DDL. Improving silica fume cement by using silane. Cem Concr Res 2000;30:1305–11.
[21] Chung DDL. Improving cement-based materials by using silica fume. J Mater Sci 2002;37:673–82.
[22] Chen P, Chung DDL. Mechanical energy dissipation using cement-based materials with admixtures. ACI Mater J 2013;110:279–90.
[23] Shokoohi S, Arefazar A, Khosrokhavar R. Silane coupling agents in polymer-based reinforced composites: a review. J Reinf Plast Compos 2008;27:473–85.
[24] ASTM C384-04. Standard test method for impedance and absorption of acoustical materials by impedance tube method. 2011.
[25] Skumiel A, Jozefczak A, Timko M, Kopcansky P, Koneracka M. The effect of a magnetic field on the absorption coefficient of ultrasonic wave in biocompatible ferrofluid. Czechoslov J Phys 2004;54(Suppl. D):D651–4.
[26] Priya M, Satish Rao BS, Ray S, Mahato KK. Prediction of absorption coefficients by pulsed laser induced photoacoustic measurements. Spectrochim Acta Part A Mol Biomol Spectrosc 2014;127:85–90.
[27] Zorebski E, Geppert-Rybczynska M, Zorebski M. Acoustics as a tool for better characterization of ionic liquids: a comparative study of 1-alkyl-3-methylimidazolium bis[(trifluoromethyl)sulfonyl]imide room-temperature ionic liquids. J Phys Chem 2013;B 117(14):3867–76.
[28] Ale B, Rousseau C. Dynamic attenuation and compressive characterization of syntactic foams. J Eng Mater Technol 2013;135(3):031007/1–031007/6.
[29] Dugan S, Arnold W. Ultrasonic absorption in fatigued materials. In: AIP Conference Proceedings 1511. Review of Progress in Quantitative Nondestructive Evaluation, vol. 32B; 2013. p. 1250–7.
[30] Hui Z, Xu F. Sound absorption properties of hemp fibrous assembly absorbers. Sen'i Gakkaishi 2009;65(7):191–6.
[31] Cavanaugh WJ, Tocci GC, Wilkes JA, editors. Architectural acoustics. 2nd ed. Wiley; 2010. p. 45.